Modeling and analyzing multi-megawatt direct-drive wind-turbine power system in offshore application: power flow and short circuit

Hung Vu Xuan[1*], *Huy* Nguyen Quang[1], and *Cuong* Nguyen Dang[2]

[1]Department of Electrical Engineering, School of Electrical and Electronic Engineering, Hanoi University of Science and Technology, Vietnam
[2]Centre of Design, Manufacturing and Testing (Satitech), Vietnam

Abstract. Renewable energy is experiencing a dramatic growth, in which wind energy plays a key role. The design technique of wind turbines must change to meet high requirements for accuracy and auto-ability. A designed wind turbine must be evaluated with various operational scenarios, while the traditional calculation method could be less effective and time-consuming. Recently, the technical calculation and simulation for electrical power system of a wind turbine are rapidly developed and show the high effectivity in analysis and optimal design. This study performs crucial simulations and analyses, including load flow and short circuit, to evaluate the design of a five-megawatt offshore wind turbine according to International Electrotechnical Commission (IEC) standards using Electrical Transient Analyzer Program (ETAP) software. The technique and methodology presented in this paper help engineers make the right decisions regarding equipment selection and design of a wind turbine's power system. Therefore, the reliability of designed wind turbine power system is improved in comparison with that of the conventionally designed one.

1 Introduction

The growing development of wind power in renewable energy sources (RES) shows its significant potential as a sustainable alternative to fossil fuels in the future. According to the Global Wind Report 2024 (Global Wind Energy Council – GWEC), the total capacity of wind power will reach 2.75 terawatts by 2030 [1]. With a long coastline and rich offshore wind resources, Vietnam is prioritizing wind power development to achieve Vietnam's ambitious goal of net zero emission by 2050. The implementation of the Vietnamese government's Power Development Plan VIII (PDP8) marks the government's commitment to driving the nation's energy transition [2].

Wind energy takes an increasingly high percentage in electrical power system, so the accurate calculation and design of wind turbine (WT) power system is highly significant for ensuring long-term operation, stability, and reliability for the power grid**.** The paper focuses

* Corresponding author: hung.vuxuan@hust.edu.vn

on implementing crucial analyses such as load flow and short circuit (harmonic analysis and low voltage ride through would be discussed in a separated paper) through the support of Electrical Transient Analyzer Program (ETAP) software. ETAP facilitates the direct modification of parameters to meet the system requirement about the power losses, enabling the selection of equipment such as transformer, circuit breaker, cable, etc. Additionally, it allows planning to generate electricity adapting to the current demand, forecast in the future, and determine the best conditions of the protection system based on simulation results. Moreover, it also offers a significant advantage in calculating accuracy and visualization compared to traditional methods. Analysis reports follow the criteria of the IEC 60038-2009 and IEC 60909.

The wind turbine used in this case study for reference has a power of five megawatts (5MW) and utilizes direct-drive permanent magnet generator for offshore application [3-5]. The turbine has a hub height of 105m and a blade diameter of 115m, Figure 1. Even though, the wind turbine in this study does not belong to the largest power group (15MW, hub height of 150m rotor diameter of 240 m) in the world but it is the biggest wind turbine in the author's country so far. The concept in this paper can be expended to apply for super high power wind turbines (>10MW). It should be mentioned that RMS line to line voltage of a MW generator is 3.2 kV for 5MW, 4.8kV for 15 MW [6].

Overall, this study contributes to analyzing wind turbine design based on the international standard through ETAP software. The rest of this work is structured as follows: Firstly, the electrical specification of a wind turbine is listed. The difference between the onshore and offshore wind turbine is presented. After that, the implementation of simulation and analysis, including load flow and short circuit, are investigated. Finally, the conclusion is given.

Fig. 1. Illustration of multi-MW wind turbine.

2 Specification parameter

2.1 Wind turbine specification

As illustrated in Figure 2, a comprehensive structure of a multi-megawatt wind turbine power system is presented. Figure 3 shows main devices, namely main transformer and circuit breakers of main and auxiliary transformer at bottom tower section of the 5MW wind turbine in this case study. The core component is a five megawatts (5MW) wind turbine generator generating electric power.

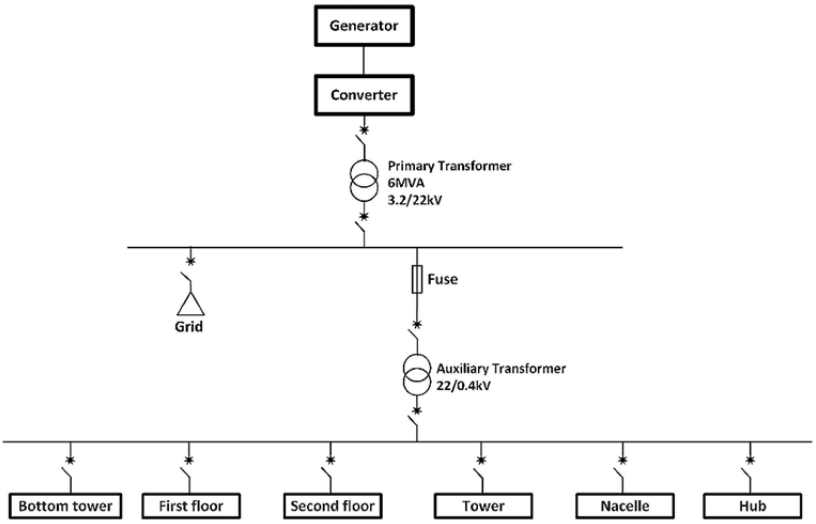

Fig. 2. Simplified structure of a 5MW wind turbine power system

Fig. 3. Some main devices of the 5MW-WT at bottom tower: (a) overview of main transformer; (b) top view of the main transformer including protecting devices; (c) SF6-circuit breaker of main transformer; (d) circuit breaker and fuse cabinet of auxiliary transformer.

Generator power is controlled by a back-to-back converter and passed through a 6MVA oil transformer (called main transformer) with parameters (short circuit voltage $u_{sc}\% = u_k\% = 6.5\%$, no load current $I_0\% = 0.4\%$), which steps up voltage to 22kV to enhance transmission efficiency. A 3-phase SF6 switchgear with rated current of 1250A and a rated short-circuit current breaking capacity of 100kA safeguards the system when overload and short-circuit, and human when operation and maintenance.

The output of the main transformer is divided into two branches. One branch connects to the power grid. The other branch steps down voltage using a 160kVA oil auxiliary transformer with parameters ($u_{sc}\% = u_k\% = 4\%$, $R_k = 16.2m\Omega$, $X_k = 41.0m\Omega$), diverting power back to the wind turbine for self-consumption. The protection for auxiliary transformer is provided by a combination of fuse with $I_{sc} = 2.6kA$ and circuit breaker. The low-voltage source then enters the distribution cabinet directing the electricity to different sections of wind turbine, namely bottom tower, first floor, second floor, tower, nacelle, and hub.

2.2 Detail load parameters

Parameters of self-consumption loads are crucial for implementing the wind turbine power system simulation on ETAP software. The accurate integration of load parameters along with the parameters of other wind turbine components (mentioned in the previous sub-section) into a completed model will significantly improve the accuracy of simulation results. In this section, the study will present the overall structure of the self-consumption system and then provide detailed parameters of devices in the offshore wind turbine.

A five-megawatt wind turbine contains several sections: Bottom tower, first floor, second floor, tower, nacelle, and hub. The bottom tower is where cooling liquid container is placed. The first floor contains a main transformer, and an auxiliary transformer with one oil pump and one redundant pump. SF6 switchgear is used to protect the system. The cooling pump circulates cooling solution from the bottom tower to the second floor to cool power electronics converter; then cooling solution returns to the first floor to cool transformers; finally goes to heat sink placed on the outside tower and comes back the tank in the bottom tower. In addition, in the first floor, there is an Uninterruptible Power Supply (UPS) with a capacity of 50kVA, which is a crucial equipment providing storage power as grid black-out for essential devices such as computer, sensors, weather station, yaw drive systems, etc., to continue operating WT in the safe mode up to three hours. Under normal operating conditions, the power supply for UPS' electronics spends 1kW. On the second floor, a back-to-back converter is the main equipment, spending 13kW for precharging and cooling, 10kW for heaters during cold weather.

A 4kW elevator is placed in the tower to easily access the nacelle for maintenance. The HVAC system plays a crucial role in regulating temperature and humidity within the specified limitation, and ensuring pressure balance in the tower. Next, in the nacelle, yaw drive systems placed are used to adjust the horizontal axis direction of wind turbine to be compatible with wind direction. The main component in the nacelle is the five-megawatt direct-drive generator with the generator's cooling system specially designed for offshore application, as illustrated in Figure 4. When generator is working, its power losses mainly include mechanical loss, copper loss in windings, iron loss in stator iron and eddy current in magnets [3, 5]. The power loss makes the generator hot. Therefore, the cooling system must be calculated for the worst situation to ensure that windings and magnets are not the over permitted temperatures [4, 7]. The generator cooling structure in Figure 4 is surveyed based on a real WT system and its datasheet. The working principle is that the inlet air goes into the generator by two fans; then hot air escaping with a flow rate of $4500m^3/h$ will be fed into the heat exchanger through two sets of ducts. When the air cools down to 35°C at the

exchanger exit, it will be blown again into the nacelle at the flow rate of 4000 m^3/h. This is the difference between onshore and offshore wind turbines. An offshore WT is a closed system to be able to work in an environment with high levels of humidity and salt. In the hub, pitch motors are Brushless DC electric motors (BLDC). Pitch drives control 3-pitch motors to the expected blade angle [8].

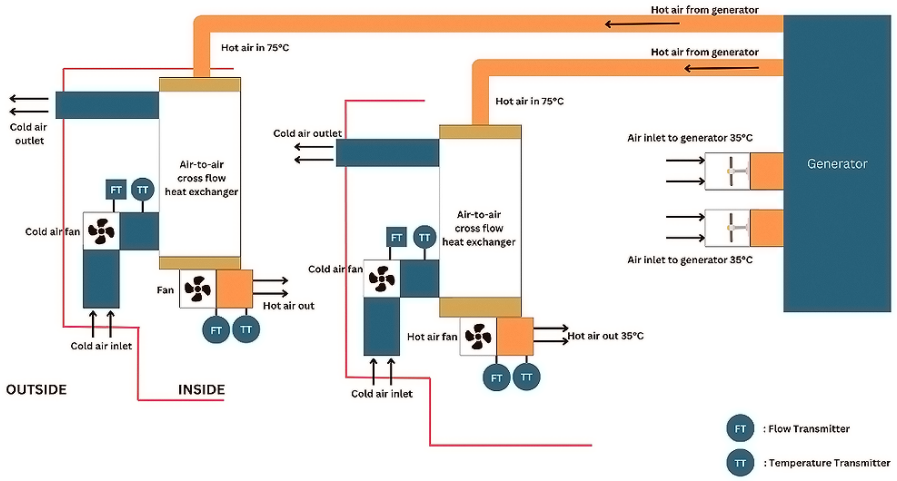

Fig. 4. Illustration of generator cooling system in wind turbine.

As shown in Table 1, loads in this wind turbine are expressed through the following parameters: Active Power (P), Power factor (PF), Apparent power (S), Utility factor (K_u), Apparent power demand max (S_{dm}), Simultaneity factor (K_s), Apparent power demand (S_d), Total apparent power demand (S_{dt}).

Table 1. Parameters of self-consumption loads in the wind turbine

		P (kW)	PF	S (kVA)	Ku	Sdm (kVA)	Ks	Sd (kVA)	Sdt (kVA)
Bottom tower	Lighting	0.34	0.9	0.40	1.00	0.40	1.00	0.40	**0.40**
1st floor	Lighting	0.34	0.9	0.40	1.00	0.40	1.00	0.40	**9.60**
	Air conditioner	3.15	0.9	3.50	0.90	3.15	1.00	3.15	
	Cooling pump	4	0.8	5.00	0.80	4.00	1.00	4.00	
	Oil circulating pump	1	0.8	1.25	0.80	1.00	1.00	1.00	
	UPS	1	1	1.05	1.00	1.05	1.00	1.05	
2nd floor	Lighting	0.34	0.9	0.40	1.00	0.40	1.00	0.40	**21.95**
	Air conditioner	3.15	0.9	3.50	0.90	3.15	1.00	3.15	
	Converter	18.4	0.8	23.00	0.80	18.40	1.00	18.40	
Tower	Lighting	1.36	0.9	1.60	1.00	1.60	1.00	1.60	**13.28**
	Tower HVAC	10.2	0.9	12.00	0.80	9.60	0.80	7.68	
	Elevator	4	0.8	5.00	0.80	4.00	1.00	4.00	
Nacelle	Lighting	0.68	0.9	0.80	1.00	0.80	1.00	0.80	**56.88**
	Nacelle HVAC	16.40	0.8	20.50	0.80	16.40	0.80	13.12	
	Generator HVAC	18	0.8	22.50	0.80	18.00	0.80	14.40	
	Meteo station	0.5	0.9	0.56	1.00	0.56	1.00	0.56	
	Six yaw system	24	0.8	30.00	0.80	24.00	1.00	24.00	
	Grease pump	4	0.8	5.00	0.80	4.00	1.00	4.00	
Hub	Pitch system	65.4	0.9	72.67	0.80	58.13	1.00	58.13	**58.13**
Total System									**160.24**

3 Methodology

Electrical Transient Analyzer Program (ETAP) version 19.0.1 was used in this study, which is a leading platform for modeling, real-time simulation, and optimizing customer electricity power systems [9]. Two analyses were conducted on this multi-megawatt direct-drive wind turbine power system, namely load flow and short circuit.

3.1 Load flow analysis

Load flow is a primary analysis used to determine voltage regulation, current flow, power loss, real and reactive power, and other system parameters under various supply and load conditions [10, 11]. By using this simulation's result, engineers can adjust the design to optimize steady-state operation [12]. Figure 5 shows the single-line diagram of the wind turbine power system that implemented load flow analysis on ETAP. This load flow study case uses the Newton-Raphson method with the maximum iteration of 99 and precision of 0.001. The results not only ensure a stable operation but also serve as an intermediate step for short-circuit analysis.

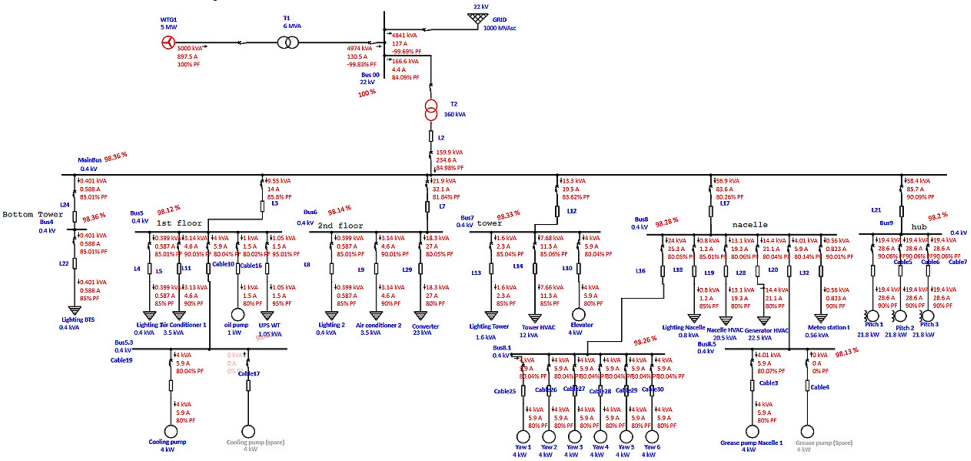

Fig. 5. Load flow simulation on ETAP.

International Standard IEC 60038-2009 defines a set of five bands that constrain the voltage for use in low-voltage and high-voltage AC electric systems. Following band one (low voltage, single & 3 phase, 50Hz, 100V to 1000V), this self-consumption network in this turbine targets achieving stable voltage operation within a +/10% range of the rated voltage [13]. As illustrated in Figure 6, the analysis identified the average bus voltage (%) within the power system. The results are 98.36%, 98.36%, 98.12%, 98.12%, 98.14%, 98.33%, 98.28%, 98.26%, 98.13%, 98.2% at the MainBus, Bus4, Bus5, Bus5.3, Bus6, Bus7, Bus8, Bus8.1, Bus8.5, Bus9, respectively. Therefore, the simulated voltage losses fall within the acceptable range and ensure a maximum 4% voltage drop supply to the final equipment. The detailed load flow report is given in Figure 6 below.

Bus		Voltage		Generation		Load		Load Flow					XFMR
ID	kV	% Mag.	Ang.	MW	Mvar	MW	Mvar	ID	MW	Mvar	Amp	%PF	%Tap
*Bus 00	22.000	100.000	0.0	-4.825	0.383	0.000	0.000	BusWT	-4.966	0.293	130.5	-99.8	
								Bus3	0.140	0.090	4.4	84.1	
Bus3	0.400	98.601	-1.0	0.000	0.000	0.000	0.000	MainBus	0.136	0.084	234.6	85.0	
								Bus 00	-0.136	-0.084	234.6	85.0	2.500
Bus4	0.400	98.355	-1.0	0.000	0.000	0.000	0.000	Bus4.1	0.000	0.000	0.6	85.0	
								MainBus	0.000	0.000	0.6	85.0	
Bus4.1	0.400	98.339	-0.9	0.000	0.000	0.000	0.000	Bus4	0.000	0.000	0.6	85.0	
Bus5	0.400	98.123	-0.9	0.000	0.000	0.000	0.000	Bus5.4	0.001	0.001	1.5	80.0	
								Bus5.5	0.001	0.000	1.5	95.0	
								MainBus	-0.008	-0.005	14.0	85.7	
								Bus5.1	0.000	0.000	0.6	85.0	
								Bus5.2	0.003	0.001	4.6	90.0	
								Bus5.3	0.003	0.002	5.9	80.0	
Bus5.1	0.400	98.107	-0.9	0.000	0.000	0.000	0.000	Bus5	0.000	0.000	0.6	85.0	
Bus5.2	0.400	97.990	-0.8	0.000	0.000	0.003	0.001	Bus5	-0.003	-0.001	4.6	90.0	
Bus5.3	0.400	98.119	-0.9	0.000	0.000	0.000	0.000	Bus 5.32	0.000	0.000	0.0	0.0	
								Bus5.31	0.003	0.002	5.9	80.0	
								Bus5	-0.003	-0.002	5.9	80.0	
Bus5.4	0.400	98.085	-0.9	0.000	0.000	0.001	0.001	Bus5	-0.001	-0.001	1.5	80.0	
Bus5.5	0.400	98.076	-0.9	0.000	0.000	0.001	0.000	Bus5	-0.001	0.000	1.5	95.0	
Bus5.31	0.400	98.026	-0.8	0.000	0.000	0.003	0.002	Bus5.3	-0.003	-0.002	5.9	80.0	
Bus 5.32	0.400	98.119	-0.9	0.000	0.000	0.000	0.000	Bus5.3	0.000	0.000	0.0	0.0	
Bus6	0.400	98.142	-0.9	0.000	0.000	0.000	0.000	MainBus	-0.018	-0.013	32.1	81.8	
								Bus6.1	0.000	0.000	0.6	85.0	
								Bus6.2	0.003	0.001	4.6	90.0	
								Bus6.3	0.015	0.011	27.0	80.0	

Fig. 6. Load flow report.

3.2 Short circuit analysis

Short circuits in the power system can cause detrimental consequences, including overheating, fire hazards, equipment damage, system disruption, financial losses, etc. ETAP facilitates mitigating the risks by calculating short-circuit current throughout the electrical system based on the IEC 60909 standards. Therefore, it enables the selection of appropriate protective equipment, such as high-voltage and low-voltage circuit breakers, fuses, and other components that can effectively detect and rapidly isolate the faulted current out of the system. Simulating the operational status of protective devices during fault conditions can also be implemented to guarantee the system's functionality.

Short-circuit faults are classified into two primary types: symmetrical fault (three-phase) and unsymmetrical fault (single line-to-ground, line-to-line, double line-to-ground). However, the three-phase short-circuit fault is the most severe fault condition due to the strongest current that flows in the system. Hence, the work will predominantly focus on calculating parameters for the worst-case (three-phase short-circuit) to ensure the system can identify the most severe condition. The results of other short-circuit faults are also presented with those four parameters through results from ETAP software. Figure 7 explains for types of short-circuit far-from-generator and short-circuit near-to generator as well as defines initial short-circuit current, peak short-circuit current [14, 15]. The short-circuit parameters are explained more detail as the following.

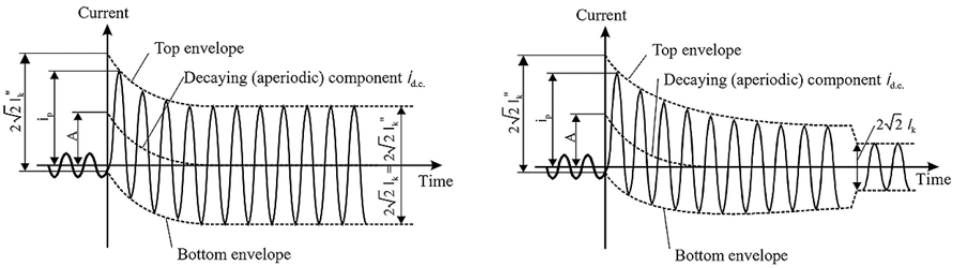

Fig. 7. Far-from-generator short circuit with constant AC component, with breaking current equals the initial symmetrical short-circuit current I_k'' (a). Near-to-generator short circuit with decaying AC component, with breaking short-circuit current is smaller than the initial symmetrical short-circuit current I_k'' (b).

- Effective value (also called root mean square value) of the Initial symmetrical short-circuit current (I_k'') is given as the following equation [14-16]:

$$I_k'' = \frac{c \cdot U_n}{\sqrt{3} \cdot Z_{sc}} = \frac{1}{\sqrt{3}} \cdot \frac{c \cdot U_n}{\sqrt{R_k^2 + X_k^2}}, \quad (1)$$

where c is the voltage factor in range of 0.9 to 1.1, U_n is the nominal voltage at the short-circuit location. Z_k is defined as the total impedance ($Z_k = R_k + j.X_k$), R_k and X_k are short circuit the resistance and reactance, respectively, as referenced in [16].

- Peak current (I_p) describes the highest value of short-circuit current from each branch:

$$I_p = \sqrt{2}.k_s.I_k'', \quad (2)$$

where k_s is the factor can be read from the graph $k_s = f(X/R)$ or $f(R/X)$, as illustrated in Figure 8, according to the IEC 60909 standard [16]. Alternatively, the k_s factor is given by:

$$k_s = 1.02 + 0.98e^{-3R/X}, \quad (3)$$

with

$$\frac{R}{X} = \frac{R_c}{X_c} \cdot \frac{f_c}{f}, \quad (4)$$

where R_c and X_c are the real part and imaginary part of equivalent impedance ($Z_c = R_c + jX_c$) at the short-circuit location for the frequency $f_c = 20Hz$ or $f_c = 24Hz$ (correspond to nominal frequency $f = 50Hz$ or $f = 60Hz$) [15].

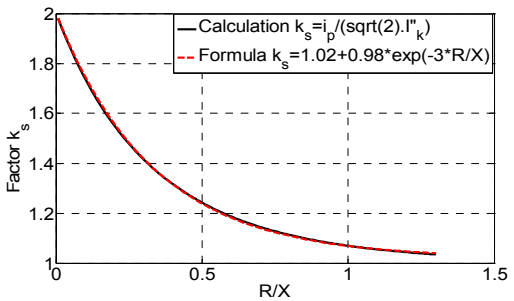

Fig. 8. Presenting the relationship of factor k_s and the ratio of R to X.

- The calculations for short circuit breaking current (I_b) consider the electrical distance between the location of the fault and the generator. For faults occurring remotely from the generator, breaking current (I_b) and initial symmetrical short-circuit current (I_k'') are equal:

$$I_b = I_k''. \tag{5}$$

For fault near-to-generator, I_b is given by:

$$I_b = \mu . I_k''. \tag{6}$$

Factor μ is contingent upon the minimum time delay (t_{min}) that adheres to the IEC 60909 standard. For each specific time point, the factor μ can be determined according to [17].

- Steady-state short-circuit current, I_k, is the root mean square value of symmetrical current and has an accuracy lower than the initial symmetrical short-circuit current. There are differences between calculating I_k in meshed networks, non-meshed networks, generator or power station at the three-phase short circuit [15].

Figure 9 depicts a three-phase balance short-circuit occurring at the main bus in the wind turbine electrical system. As illustrated, it provides valuable information about short-circuit related to the main bus and other buses. Thus, researchers and engineers can gain valuable insights into faults and implement necessary protective measures to mitigate potential disruptions within wind turbine power systems.

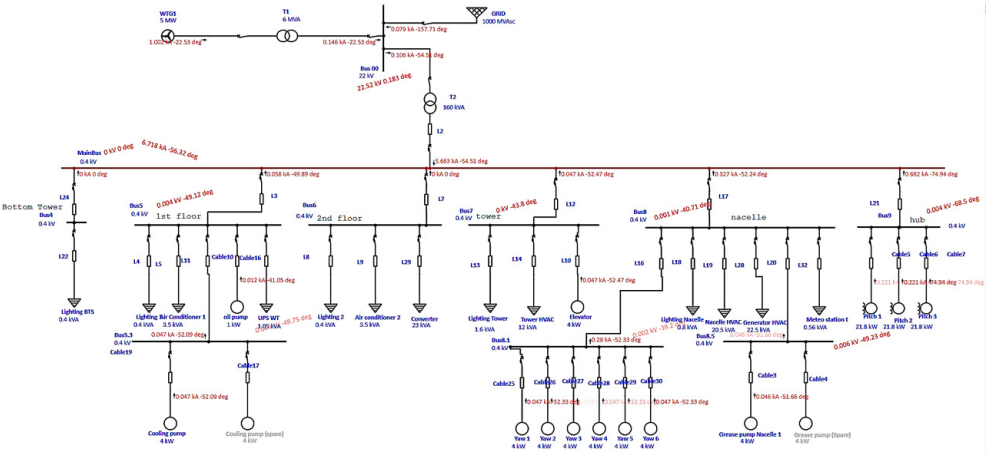

Fig. 9. Short circuit simulation with fault on main bus (IEC 60909 standard).

The short-circuit calculation results on ETAP presented in Tables 2 to 9 correspond to four fault types, including three-phase, single line-to-ground (L-G), line-to-line (L-L), double line-to-ground (L-L-G) when the fault location at Bus0, Mainbus, Bus4, Bus5, Bus6, Bus7, Bus8, Bus9 [18].

Table 2. Short-circuit fault at the Bus0 (After the main transformer)

Fault Current	3-phase	L-G	L-L	L-L-G
Initial symmetrical current I"k (kA, rms)	26.435	5.855	22.852	22.916
Peak current Ip (kA)	57.552	12.738	49.719	49.859
Steady-state current Ik (kA, rms)	26.597	5.855	22.852	22.916

Table 3. Short-circuit fault at the Mainbus

Fault Current	3-phase	L-G	L-L	L-L-G
Initial symmetrical current I"k (kA, rms)	6.718	6.010	5.734	6.551
Peak current Ip (kA)	11.142	9.967	9.508	10.864
Steady-state current Ik (kA, rms)	6.253	6.010	5.734	6.551

Table 4. Short-circuit fault at the Bus4 (Bottom tower)

Fault Current	3-phase	L-G	L-L	L-L-G
Initial symmetrical current I"k (kA, rms)	5.514	4.412	4.726	5.418
Peak current Ip (kA)	8.334	6.668	7.142	8.188
Steady-state current Ik (kA, rms)	5.261	4.412	4.726	5.418

Table 5. Short-circuit fault at the Bus5 (First floor)

Fault Current	3-phase	L-G	L-L	L-L-G
Initial symmetrical current I"k (kA, rms)	3.797	2.625	3.260	3.608
Peak current Ip (kA)	5.507	3.807	4.728	5.232
Steady-state current Ik (kA, rms)	3.659	2.625	3.260	3.608

Table 6. Short-circuit fault at the Bus6 (Second floor)

Fault Current	3-phase	L-G	L-L	L-L-G
Initial symmetrical current I"k (kA, rms)	5.200	4.054	4.461	5.085
Peak current Ip (kA)	7.773	6.060	6.668	7.600
Steady-state current Ik (kA, rms)	4.988	4.054	4.461	5.085

Table 7. Short-circuit fault at the Bus7 (Tower)

Fault Current	3-phase	L-G	L-L	L-L-G
Initial symmetrical current I"k (kA, rms)	6.399	5.573	5.466	6.278
Peak current Ip (kA)	10.340	9.004	8.831	10.143
Steady-state current Ik (kA, rms)	5.990	5.573	5.466	6.278

Table 8. Short-circuit fault at the Bus8 (Nacelle)

Fault Current	3-phase	L-G	L-L	L-L-G
Initial symmetrical current I"k (kA, rms)	6.490	5.677	5.536	6.353
Peak current Ip (kA)	10.573	9.248	9.019	10.349
Steady-state current Ik (kA, rms)	6.047	5.677	5.536	6.353

Table 9. Short-circuit fault at the Bus9 (Hub)

Fault Current	3-phase	L-G	L-L	L-L-G
Initial symmetrical current I"k (kA, rms)	6.340	5.458	5.419	6.254
Peak current Ip (kA)	10.310	8.875	8.811	10.169
Steady-state current Ik (kA, rms)	5.926	5.458	5.419	6.254

4 Conclusion

Our paper has utilized ETAP software as a power tool for simulating and implementing load flow and short-circuit analysis for a multi-megawatt wind turbine in offshore application. By examining various aspects of wind turbine power system through simulation, our comprehensive analysis contributes to the development of renewable energy technology. Result is summed as follows.

- This study has provided a detailed description of a multi-megawatt wind turbine's electrical system and pointed out the difference between offshore and onshore wind turbine structures.

- Through power flow analysis, load flow is indicated by voltage, current, active and reactive power, power factors, etc. Based on IEC 60038-2009 standards, this study evaluated average bus voltage and used simulation result to optimize power system design of wind turbine.
- The outcomes from short-circuit analysis play a crucial role in mitigating risks by calculating essential parameters corresponding to four types of short-circuit fault complying with the IEC 60909 standard. It ensures that the system operates functionally even in the worst-case condition.
- The study emphasizes the flexibility of ETAP software in surveying and manipulating parameters more accurately compared to conventional manual calculation methods.

In the future, this work will expand its scope for larger power wind turbines, aiming to establish a general rule about cable size, capacity, motor parameter selection, etc., and conduct other related analyses to evaluate wind turbine's power system comprehensively.

This research is funded by the Hanoi University of Science and Technology (HUST) under project number T2020-SAHEP-002.
The author would like to thank to Setec Electronics & Wind Power GmbH, Darwind B.V, Getec Ltd for providing some facilities for this study.

References

1. G. W. E. Council, Global Wind Report 2024, (2024)
2. W. PWC, Vietnam's Eighth National Power Development Plan (PDP VIII), Available: https://www.pwc.com/vn/en/publications/2023/230803-pdp8-insights.pdf. (Accessed on 05 04 2024)
3. H. V. Xuan, D. Lahaye, S. O. Ani, H. Polinder, J. Ferreira, *Electrical generators for maritime application*, in Proceeding of the Electrical Machines and Systems (ICEMS), (2011)
4. Hung Vu Xuan, *A method for derating power of a MW direct-drive wind turbine permanent magnet generator as over allowable working temperature*, in Proceeding of the E3S Web Conference, (2023)
5. H. V. Xuan; S. O. Ani; D. Lahaye; H. Polinder; J. A. Ferreira, Validation of non-linear dynamic FEM model for design of PM machines with concentrated windings in ship application, (2011)
6. Gaertner and others, Definition of the IEA 15-Megawatt Offshore Reference Wind, Golden, CO: National Renewable Energy Laboratory, (2020)
7. H. Vu Xuan, Guidelines of Effective Thermal Modeling of an Outer Rotor PM Machine with Concentrated Windings, in Proceedings of the 2022 International Conference on Communications, Information, Electronic and Energy Systems (CIEES), Veliko Tarnovo, Bulgaria, pp. 1-7, (2022), DOI: 10.1109/CIEES55704.2022.9990783.
8. U. Ritschel; and M. Beyer, *Yaw and Pitch System*, in Proceedings of the Designing Wind Turbines, Springer, Cham, (2022)
9. ETAP, Operation Technology Inc, Available: https://etap.com/home. (Accessed on May 2024)
10. Mohammad Nurul Absar; Md Fokhrul Islam; Ashik Ahmed, Power quality improvement of a proposed grid-connected hybrid," Heliyon, (2023)

11. S. Kumar, M. S. Narayana, B. Naidu, G. S. Reddy, Optimal Power flow for IEEE-9 Bus System, International Journal of Recent Technology and Engineering, vol. **7**, no. 6S, p. 368, (2019)
12. O.M. Mohamed; D. Felix Amankwah; B. Benjamin, Integration of multiple distributed solar PV (DSP) into the grid: The case of the distribution network in Freetown, Sierra Leone, Solar Compass, (2024)
13. Eyad Almaita; Emad Abdelsalam; Fares Almomani; Hamza Nawafah; Fadwa Kassem; Saleh Alshkoor; Maan Shloul, Impact study of integrating solar double chimney power plant into electrical grid, Energy, (2023)
14. IEC 60909:0-4. Short circuit current calculation in three-phase AC systems, IEC, (2002)
15. M. Eremia; M. Shahidehpour, Handbook of Electrical Power System Dynamics: Modeling, Stability, and Control, IEEE, (2013)
16. D. Bandaru, S. R. Sura, J. K. Bokam and K. A. Kumar, Methods for Short Circuit Analysis in ANSI and IEC Standards, International Journal of Mechanical Engineering, vol. 7, no. 2, p. 2643, (2022)
17. W. Pacbasics, IEC 60909: 'Near' Generator Short Circuit Calculation, Available: https://pacbasics.org/iec-60909-near-generator-short-circuit-calculation/. (Accessed 25 5 2024)
18. D. S. Kumari, C. Reddy, *Transient Stability Analysis of a Combined Cycle Power Plant Using Etap Software*, in Proceedings of the 2017 IEEE 7th International Advance Computing Conference (IACC), Hyderabad, India, (2017)